

See discussions, stats, and author profiles for this publication at: <https://www.researchgate.net/publication/229063418>

Coherent Microscopic Picture for Urea-Induced Denaturation of Proteins

ARTICLE in THE JOURNAL OF PHYSICAL CHEMISTRY B · JULY 2012

Impact Factor: 3.3 · DOI: 10.1021/jp304114h · Source: PubMed

CITATIONS

14

READS

32

5 AUTHORS, INCLUDING:



[Zaixing Yang](#)

Soochow University (PRC)

25 PUBLICATIONS 159 CITATIONS

SEE PROFILE



[Peng Xiu](#)

Zhejiang University

50 PUBLICATIONS 627 CITATIONS

SEE PROFILE



[Lan Hua](#)

University of California, San Francisco

13 PUBLICATIONS 838 CITATIONS

SEE PROFILE



[Zhou Ruhong](#)

IBM

133 PUBLICATIONS 5,910 CITATIONS

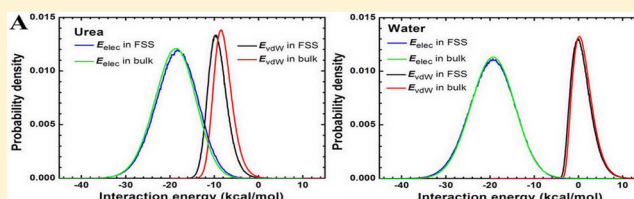
SEE PROFILE

Coherent Microscopic Picture for Urea-Induced Denaturation of Proteins

Zaixing Yang,^{†,‡} Peng Xiu,[†] Biyun Shi,[‡] Lan Hua,[§] and Ruhong Zhou^{*,†,||}[†]Department of Engineering Mechanics, and Soft Matter Research Center, Zhejiang University, Hangzhou 310027, China[‡]Bio-X Lab, Department of Physics, Zhejiang University, Hangzhou 310027, China[§]Department of Pharmaceutical Chemistry, University of California at San Francisco, San Francisco, California 94158, United States^{||}Computational Biology Center, IBM Thomas J. Watson Research Center, 1101 Kitchawan Road, Yorktown Heights, New York 10598, United States

S Supporting Information

ABSTRACT: In a previous study, we explored the mechanism of urea-induced denaturation of proteins by performing molecular dynamics (MD) simulations of hen lysozyme in 8 M urea and supported the “direct interaction mechanism” whereby urea denatures protein via dispersion interaction (Hua, L.; Zhou, R. H.; Thirumalai, D.; Berne, B. J. *Proc. Natl. Acad. Sci. U.S.A.* **2008**, *105*, 16928). Here we perform large scale MD simulations of five representative protein/peptide systems in aqueous urea to investigate if the above mechanism is common to other proteins. In all cases, accumulations of urea around proteins/peptide are observed, suggesting that urea denatures proteins by directly attacking protein backbones and side chains rather than indirectly disrupting water structure as a “water breaker”. Consistent with our previous case study of lysozyme, the current energetic analyses with five protein/peptide systems reveal that urea’s preferential binding to proteins mainly comes from urea’s stronger dispersion interactions with proteins than with bulk solution, whereas the electrostatic (hydrogen-bonded) interactions only play a relatively minor (even negative) role during this denaturation process. Furthermore, the simulations of the peptide system at different urea concentrations (8 and 4.5 M), and with different force fields (CHARMM and OPLSAA) suggest that the above mechanism is robust, independent of the urea concentration and force field used. Last, we emphasize the importance of periodic boundary conditions in pairwise energetic analyses. This article provides a comprehensive study on the physical mechanism of urea-induced protein denaturation and suggests that the “dispersion-interaction-driven” mechanism should be general.



INTRODUCTION

Urea is a strong denaturant for proteins.¹ Despite extensive studies,^{2–33} the underlying molecular mechanism of urea-induced denaturation of proteins still remains somewhat controversial.^{6,21,23,28} From earlier free energy transfer experiments,^{3,34} it is known that the solubility of most hydrocarbons and protein side chain analogues increase upon the transfer from water to aqueous urea solution. Thus, the urea denaturation mechanism can be understood loosely from the thermodynamic arguments. Transfer of the protein native state in water to urea solution lowers the free energy of the native state because of a net favorable interaction of urea with surface-exposed groups; the free energy change is even more favorable for transfer of the denatured state from water to urea because of the larger number of denatured state surface-exposed groups binding preferentially to urea. These changes result in a smaller free energy gap (ΔG) between the native and denatured states in urea compared to that in water, thus causing the protein destabilization in urea solution. However, at the molecular level the picture is far from clear. Generally speaking, the denaturing power of urea has been explained by two very different

molecular mechanisms: the “direct” and “indirect” interaction mechanisms. The “indirect” mechanism suggests that urea denatures protein either through disrupting the structure of water, which in turn weakens the hydrophobic interaction and promotes the solvation of hydrophobic groups,^{2–9} or through modifying the lifetime or strength of the hydrogen bond between water and protein, which in turn causes the surrounding water to interact more efficiently and strongly with the protein.^{10–12,35} The “direct” mechanism, on the other hand, suggests that urea unfolds proteins through its direct electrostatic/dispersion interactions with protein.^{13–32} In addition to these two general mechanisms, there is a compromising view that both direct and indirect mechanisms can be important in urea-induced protein denaturation,^{7–12,33,35} and these two different mechanisms may be strongly related.^{9,10,35}

Received: April 28, 2012

Revised: June 28, 2012

Published: July 10, 2012

In recent years, there is growing evidence supporting the “direct” mechanisms.^{15–32,36,37} Within this framework, however, the dominant driving force of the denaturation process is still a subject of considerable debate. Traditional views suggest that urea denatures proteins through strong hydrogen bonds or other electrostatic interactions with backbone and/or polar residues.^{13–21,37} In contrast, our previous study²⁷ based on molecular dynamics (MD) simulations of hen lysozyme in 8 M urea indicated that the protein unfolding is induced by the preferential binding of urea to protein, since the dispersion interaction is stronger between urea and protein than between protein and water. A “dry molten globule” transient state was predicted in our simulation for the early stage of denaturation in urea, i.e., intrusion of urea before water into the hydrophobic core of protein,²⁷ which was later observed directly by FRET and far-UV CD spectra.³⁸ Our subsequent studies^{29–31} based on model systems also implied that the preferential attractive van der Waals (vdW) interactions of urea with hydrophobic wall over water should be responsible for the “dry globule” and subsequent protein denaturation. Apart from the above two essential viewpoints, some works^{22,23} support a combination of electrostatic and vdW interactions as the dominant driving force of denaturation.

As mentioned above, our previous work had illustrated the dispersion-driven-mechanism of urea-induced protein denaturation through the case study of lysozyme. One may wonder if this mechanism is unique to the specific proteins or sensitive to urea concentration and force field used in the simulation. Thus, the current study focuses on the generality and robustness of this mechanism. On the basis of MD simulations, we repeat our energetic calculations for five representative protein/peptide systems, namely, lysozyme (mainly α -helix protein), human γ D-Crystallin (mainly β -sheet protein), ubiquitin (α/β protein), chymotrypsin inhibitor 2 (CI2, a small sized α/β protein, which can hardly hold enough urea molecules in its hydrophobic core to form a dry globule), and a small amyloid- β peptide fragment (NFGAIL). We find that the underlying mechanisms of urea-induced denaturation for these proteins/peptide are consistent, suggesting that the “dispersion-interaction-driven” mechanism should be common for all proteins. Furthermore, the simulations of the peptide system at different urea concentrations (8 and 4.5 M) and with different force fields (CHARMM and OPLSAA) suggest that the above mechanism is independent of urea concentration and force field used. Finally, we emphasize the importance of periodic boundary conditions (PBC) in pairwise energetic analyses. The present study provides a coherent microscopic picture for urea-induced denaturation of proteins.

■ COMPUTATIONAL MODELS AND METHODS

In this study, we performed simulations of five representative proteins/peptide solvated in urea solution with high urea concentration (~ 8 M): hen egg-white lysozyme (W62G mutant), human γ D-Crystallin, ubiquitin, chymotrypsin inhibitor 2 (CI2), and a small amyloid- β peptide fragment (NFGAIL), following our previous similar protocols.^{39–43} All initial structures have been taken from the crystal structure deposited in the Protein Data Bank, with PDB IDs of 193L, 1HK0, 1UBQ, 1TM1, 1YPC, and 2KIB for the wild-type lysozyme, γ D-Crystallin, ubiquitin, CI2, and NFGAIL peptide, respectively. These simulations were performed using the NAMD2MD program⁴⁴ with the all-atom CHARMM force field⁴⁵ for proteins and urea. A slightly modified TIP3P⁴⁶ water

model was used for water. In addition, in order to address the question of whether the obtained molecular mechanism is dependent on the concentration of urea or the force field used, we also performed simulations of NFGAIL peptide solvated in urea solution with another urea concentration (4.5 M), using both CHARMM and OPLSAA⁴⁷ force fields, with the GROMACS-4.0.7⁴⁸ package. [Here another molecular dynamics package GROMACS is used instead of implementing the OPLSAA force field into the NAMD2 package, partly to avoid the less tested OPLSAA force field in NAMD2 (NAMD2 simulations mostly done with the CHARMM force field) and partly to further validate the current dependence study with yet another package, which should presumably be more convincing in terms of the generality of the predicted mechanism from various simulations.] When the OPLSAA force field was used for the peptide, the OPLS urea model^{49,50} and TIP3P⁵¹ water model were used. All production MD simulations were performed under NPT ensemble, with both temperature and pressure controlled by the Berendsen methods, and considering that the human γ D-Crystallin is highly stable at physiological temperature,^{52,53} the simulation of this protein was performed at high temperature (380 K) and 1 atm. The simulations for other systems were performed at 310 K and 1 atm. During the GROMACS MD runs, the LINCS algorithm⁵⁴ was used to constrain the lengths of all bonds and the water molecules were restrained using the SETTLE algorithm.⁵⁵ In NAMD, bonds were constrained by SHAKE.⁵⁶ A time step of 2 fs was used. The particle-mesh Ewald (PME) method⁴⁷ was applied to treat the long-range electrostatic interactions, and a typical cutoff of 12 Å was used for van der Waals interactions. PBC were applied in all directions. The simulation lengths are 1 μ s for the lysozyme system, 100+ ns each for other protein systems, and 20 ns each for all NFGAIL peptide systems. The detailed sets of simulations are listed in Table 1.

Table 1. Summary of the Sets of Simulations^a

protein/ peptide	force fields	C_{urea} (M)	N_{urea}	N_{water}	box size (Å)
lysozyme	CHARMM	8	1811	7799	73.1 × 73.1 × 73.1
γ D-Crystallin	CHARMM	8	1775	7644	74.2 × 74.2 × 74.2
CI2	CHARMM	8	1441	6340	71.1 × 72.8 × 59.9
ubiquitin	CHARMM	8	1575	6722	68.5 × 69.4 × 68.1
NFGAIL	CHARMM	8	235	1013	36.5 × 36.5 × 36.5
NFGAIL	CHARMM	4.5	137	1296	36.8 × 36.8 × 36.8
NFGAIL	OPLSAA	4.5	289	2737	47.5 × 47.5 × 47.5

^a C_{urea} denotes the urea concentration; N_{urea} and N_{water} denote the number of urea and water molecules of the system. For lysozyme and CI2 systems, 8 and 2 Cl[−] counterions were added to neutralize the solvated systems, respectively. All systems were set up following a previous used method for lysozyme system.²⁷

■ RESULTS AND DISCUSSION

Mechanisms of Urea-Induced Protein Denaturation for Different Proteins. During the given simulation times, lysozyme undergoes global unfolding and finally exhibits a highly extended conformation, whereas some other proteins only undergo partial unfolding (see Figure S1 in the Supporting Information for details); the NFGAIL peptide changes from a compact conformation to an extended one. Nevertheless, the obtained trajectories are believed to be long enough for the current study, since our focus is on the physical mechanism of

urea-induced protein denaturation, rather than the complete protein unfolding process. We first investigate the influence of urea on the solvation condition of proteins by computing the ratio, $\rho_{w/u}$, which is defined as the number of water to urea molecules in the first solvation shell (FSS). [FSS is defined as a 4 Å thick solvation shell from any heavy atom (non-hydrogen atom) of protein.⁵⁷ A solvent is viewed as inside the FSS of the protein when any of its heavy atoms enters the FSS region.] We note here that this FSS definition is slightly more strict than that in our previous study²⁷ where the FSS is defined as a 5 Å thick solvation shell from any atom of a protein (including hydrogen atoms). Consistent with our previous studies, in all cases, we observe that urea molecules simultaneously accumulate around proteins' backbones and side chains by displacing water from the FSS. For example, for lysozyme in 8 M urea, $\rho_{w/u}$ around protein surface drops from ~ 4.3 ($\rho_{w/u}$ in bulk) to ~ 2.7 in a very short period of time (~ 1 ns, during the equilibration), and further drops to ~ 2.0 after about 40 ns. The changes in $\rho_{w/u}$ for other protein/peptide systems is similar: after a rapid decrease, $\rho_{w/u}$ reaches relatively stable values, roughly 2.3, 3.0, 2.1, and 2.1 for human γ D-Crystallin, ubiquitin, CI2, and NFGIL peptide in 8 M urea, respectively; these values are 3.8 and 2.8 for NFGIL in 4.5 M urea with CHARMM and OPLSAA force fields, respectively ($\rho_{w/u}$ is ~ 9.5 in bulk for 4.5 M urea system). The accumulations of urea around proteins in turn trigger the unfolding of proteins, indicating that urea denatures proteins by directly attacking protein backbones and side chains rather than disrupting water structure as a "water breaker".

The above phenomena can be explained from an energetic perspective. We have computed the nonbonded interactions (including both vdW and electrostatic) between each urea/water in the FSS of the proteins and in bulk (defined as 6 Å away from any heavy atom of protein) with the rest of the system. In the energetic calculations, a spherical cutoff of 13 Å was used for vdW interactions, and no cutoff is used for electrostatic interactions; PBC are taken into account. Figure 1 shows the interaction energy distributions of urea/water in the FSS of proteins and in bulk. In all five cases, electrostatic energy distributions of urea in protein FSS (referred to as "surface urea") nearly overlap with those of the bulk urea. However, the vdW energy distributions of the surface urea clearly shift leftward (toward the lower energy region) compared to those of the bulk urea; the shifts in peak positions are about 1.23, 1.28, 0.71, 0.82, and 0.59 kcal/mol for lysozyme, γ D-Crystallin, ubiquitin, CI2, and NFGIL peptide, respectively (see left panel of Figure 1). On the other hand, water in proteins' FSS (referred to as "surface water") has very similar distributions in both electrostatic and vdW interaction energies as compared to those in bulk water.

For the convenience of comparison, Table 2 lists the differences in the average interaction energies for a solvent (urea/water) in protein FSS and in bulk based on the detailed energy profiles shown in Figure 1. When a bulk urea approaches the protein surface, it loses electrostatic interaction energy (0.16–0.40 kcal/mol) in most cases (all except for ubiquitin system), which challenges the hydrogen-bonding-driven mechanism^{13–21,37} proposed previously; however, the surface urea gains considerable vdW interaction energy (0.59–1.30 kcal/mol) which overcompensates for the penalty in electrostatic interactions. In all cases, urea gains more energy than water when moving from the bulk to the FSS. In the extreme case of the NFGIL peptide, the changes in total

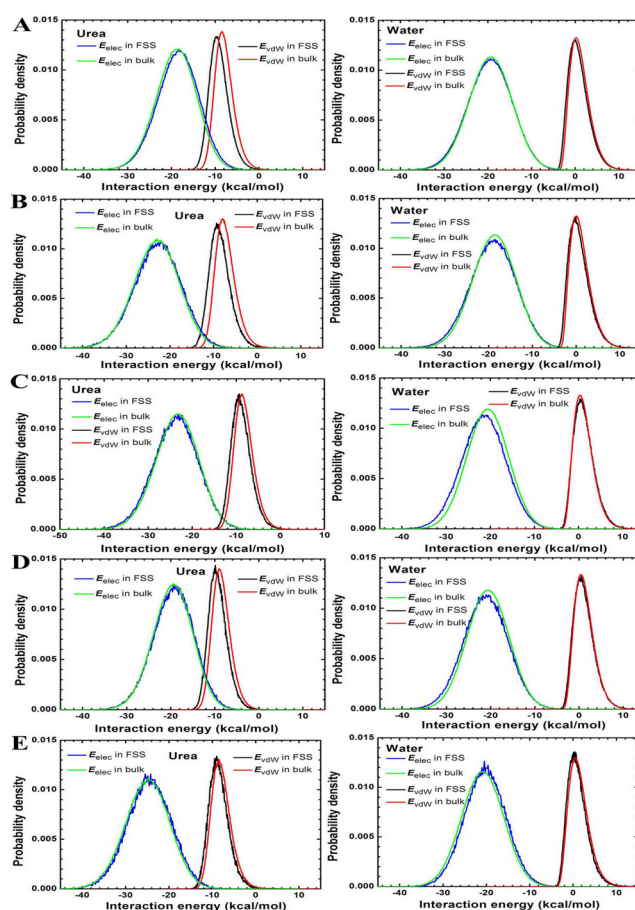


Figure 1. Interaction energy distributions for urea (left panel) and water (right panel) in the first solvation shell (FSS) of proteins and in bulk. Panels A–E denote the cases for lysozyme, γ D-Crystallin, ubiquitin, CI2, and NFGIL peptide, respectively. E_{elec} and E_{vdW} denote the electrostatic and vdW interactions of a solvent with the rest of the system.

Table 2. Differences in the Average Interaction Energies (kcal/mol) for a Solvent (Urea/Water) in the First Solvation Shell of Proteins vs in Bulk, with the Rest of the System^a

protein	solvent	ΔE_{elec}	ΔE_{vdW}	ΔE_{total}
lysozyme	urea	0.40	−1.23	−0.83
	water	−0.15	−0.34	−0.49
γ D-Crystallin	urea	0.24	−1.30	−1.06
	water	−0.24	−0.31	−0.55
ubiquitin	urea	−0.29	−0.66	−0.95
	water	−0.90	0.04	−0.86
CI2	urea	0.16	−0.83	−0.67
	water	−0.52	−0.14	−0.66
NFGIL	urea	0.40	−0.59	−0.19
	water	0.58	−0.35	0.23

^a ΔE_{elec} , ΔE_{vdW} , and ΔE_{total} denote the differences in electrostatic, vdW, and total interaction energies, respectively.

interaction energy are negative for urea but positive for water, meaning that water even loses enthalpy when moving from the bulk to the FSS due to more hydrophobic nature of the peptide, in addition to the loss in entropy due to its lower mobility on the peptide surface. Overall, urea gains more interaction energy than water, which is responsible for the urea's preferential binding to proteins over water.

Table 3. Distributions of Polar, Nonpolar, Basic, and Acidic Residues in Ubiquitin and CI2 Proteins, as well as the Ratio of the Number of Water to Urea Molecules ($\rho_{w/u}$) and the Average Electrostatic Energies of a Water (E_{elec} in kcal/mol) in the First Solvation Shell of Side Chains with the Rest of the System

proteins		polar	nonpolar	basic	acidic	total
ubiquitin	percentage	34.2%	36.8%	14.5%	14.5%	100%
	$\rho_{w/u}$	2.5	2.1	3.1	4.8	3.0
	E_{elec}	−21.05	−20.40	−21.72	−23.04	−21.53
CI2	percentage	18.8%	53.1%	15.6%	12.5%	100%
	$\rho_{w/u}$	2.0	1.7	3.1	4.4	2.1
	E_{elec}	−20.64	−20.35	−21.78	−22.66	−21.13

Note that the differences in total interaction energy for water are very close to those for urea in CI2 and ubiquitin cases (see Table 2) and that one may doubt that why urea can displace water and accumulate around proteins. A closer examination of CI2 and ubiquitin cases indicates that the relatively stronger interaction energies that these surface water molecules have as compared to other cases mainly come from the more favorable electrostatic interactions. Both ubiquitin and CI2 have unusually large surface charges (charged residues). We perform detailed analyses of $\rho_{w/u}$ and water's electrostatic interactions in different regions of these two proteins by decomposing them into four categories in terms of the hydrophobicity of the residue side chains. The results are presented in Table 3. We find that water gains more electrostatic interaction energies around the acidic (negatively charged) and basic (positively charged) residues, with acidic residues being most energetically favorable. Meanwhile, $\rho_{w/u}$ around acidic residues is close to that of bulk value (~ 4.3); around basic residues it is moderate (3.1), and around noncharged residues it is small (1.7–2.5), with $\rho_{w/u}$ around nonpolar residues being the smallest (1.7 and 2.1). These results suggest that urea's aggressive behavior for various types of amino acids is selective: urea mostly prefers to attack nonpolar residues, then the polar residues, and then the basic residues; it appears that urea unfavors binding with acidic residues. These findings are qualitatively consistent with those of Stumpe et al.²⁴ and imply that the dominate driving force for protein denaturation by urea is not through the hydrogen bonding or other electrostatic interactions. Both CI2 and ubiquitin have a relatively high proportion of charged residues especially acidic residues compared to other proteins/peptide (the proportions of acidic and basic residues are 14.5% and 14.5%, respectively, for ubiquitin, 12.5% and 15.6%, respectively, for CI2, 7% and 13.1%, respectively, for lysozyme, and 12.7% and 12.7%, respectively, for γ D-Crystallin, and there is no charged residue on the NFGAIL peptide), and therefore, ΔE_{total} for water is close to that for urea (see Table 2). These results indicate that urea denatures proteins preferably through the attack of nonacidic residues, particularly the noncharged residues. Moreover, we note that γ D-Crystallin, ubiquitin, and CI2 only undergo partial unfolding and their hydrophobic cores are largely undisrupted during the given simulation times, so it is reasonable to expect that the difference in ΔE_{total} between urea and water for these protein systems should be more distinct if the entire unfolding trajectories are employed, in view of the fact that the nonpolar residues in hydrophobic cores favor urea rather than water.

Mechanisms of Urea-Induced Protein Denaturation with Different Urea Concentrations and Force Fields. In the previous section, by taking five representative protein/peptide systems as examples, we have demonstrated that the urea unfolds proteins/peptide via direct dispersion-driven

interactions. In the following, we investigate if the above mechanism is sensitive to urea concentrations and force fields used. We chose a relatively small system, the NFGAIL peptide system, for illustration. In addition to the simulation at high urea concentration (8 M) with CHARMM force field, we also performed simulations of that peptide at moderate urea solution (~ 4.5 M), with both CHARMM and OPLSAA force fields. We observe that the NFGAIL peptide changes from a compact conformation to an extended one (its end-to-end distance increases ~ 2 Å). Figure 2 shows the interaction energy

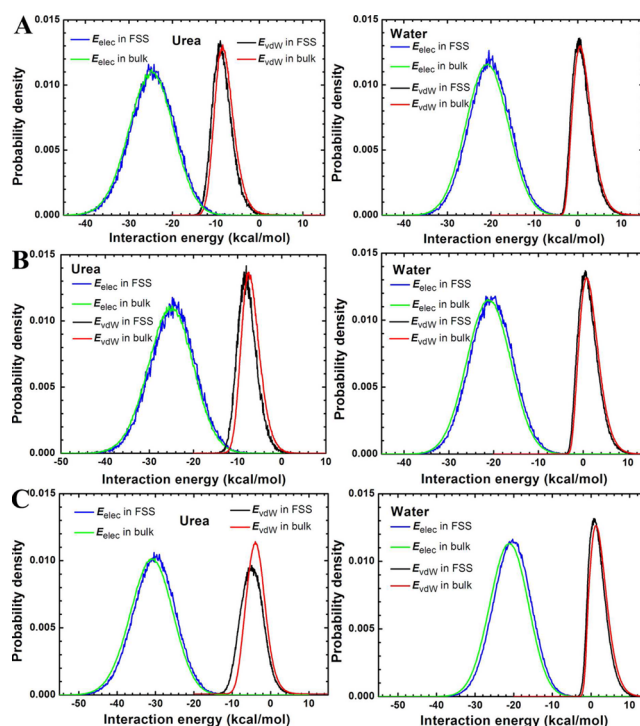


Figure 2. Interaction energy distributions for urea (left panel) and water (right panel) in the first solvation shell (FSS) of NFGAIL peptide and in bulk. Panels A and B denote the cases for 8 and 4.5 M urea systems, respectively, with CHARMM force field; panel C denotes the case for 4.5 M urea system with OPLSAA force field. E_{elec} and E_{vdW} denote the electrostatic and vdW interactions of a solvent with the rest of the system, respectively.

distributions of urea/water in the peptide FSS and in bulk. In all three cases, although the corresponding peak magnitudes and positions are different, the tendency and underlying mechanism are essentially the same: only the vdW interaction distribution for surface urea clearly departs from (i.e., shifting leftward) the corresponding bulk distribution; other distributions for both surface solvents (urea and water) nearly overlap

with the corresponding bulk distribution, indicating that it is the strong dispersion interaction between urea and peptide that drives urea onto the peptide surface, which in turn changes the conformation of peptide from compact to extended.

Table 4 shows the differences in the average interaction energies for a solvent in the FSS of peptide and in bulk.

Table 4. Differences in Average Nonbonded Interaction Energies (kcal/mol) for a Solvent in the First Solvation Shell of NFGAIL Peptide vs in Bulk Using Different Urea Concentrations (C_{urea}) and Force Fields^a

C_{urea} (M)	force fields	solvent	ΔE_{elec}	ΔE_{vdW}	ΔE_{total}
8	CHARMM	urea	0.40	−0.59	−0.19
		water	0.58	−0.36	0.23
4.5	CHARMM	urea	0.48	−0.89	−0.41
		water	0.59	−0.40	0.19
4.5	OPLSAA	urea	0.74	−1.06	−0.32
		water	0.80	−0.48	0.32

^a ΔE_{elec} , ΔE_{vdW} , and ΔE_{total} denote the differences in electrostatic, vdW, and total interaction energies, respectively.

Regardless of urea concentrations and force fields used, when approaching the peptide surface, both urea and water lose electrostatic interaction energies, but urea gains more vdW interaction energy than water; overall, urea gains interaction energy whereas water loses. The above results suggest that the dispersion-driven-mechanism is robust, i.e., independent of urea concentrations and the force fields used. It should also be noted that the replacement of water molecules by larger urea molecules in the FSS of proteins (on average each urea molecule can replace ~ 2.5 water molecules) is favorable in general because of an overall solvent entropy gain.

Importance of Periodic Boundary Conditions on Energetic Calculations. In this section, we would like to emphasize the importance of periodic boundary conditions (PBC) in pairwise energetic analyses, as to our knowledge, ignoring PBC is a frequent overlook in these type of energetic calculations. We compare the nonbonded interaction energy distributions of a solvent with or without PBC, using the lysozyme and NFGAIL peptide as examples. As shown in Figure 3, the interaction energy distributions calculated with PBC are notably different from those calculated without PBC in terms of shape of distribution as well as position and magnitude of peaks.

Table 5 compares the average interaction energies of a solvent, calculated with and without PBC. Consistent with the distribution in Figure 3, the calculated interaction energies with PBC are notably different from those without PBC. For example, when urea approaches the protein/peptide surface, its actual change in electrostatic interaction energy is positive; but if the PBC is ignored, the resulting value is negative. Moreover, for NFGAIL peptide system, it is clear that it is the dispersion interaction that drives urea onto the peptide surface; but if the PBC is ignored, both electrostatic and dispersion interactions are responsible for the accumulation of urea around the peptide. In our previous report,²⁷ PBC was ignored in these pairwise energetic calculations for lysozyme, so the resulting data are slightly off. Despite these slightly off data (which are corrected here), the main point of its conclusion does not change; that is, the urea-induced denaturation of proteins mainly results from the stronger dispersion interaction of urea with protein than water.

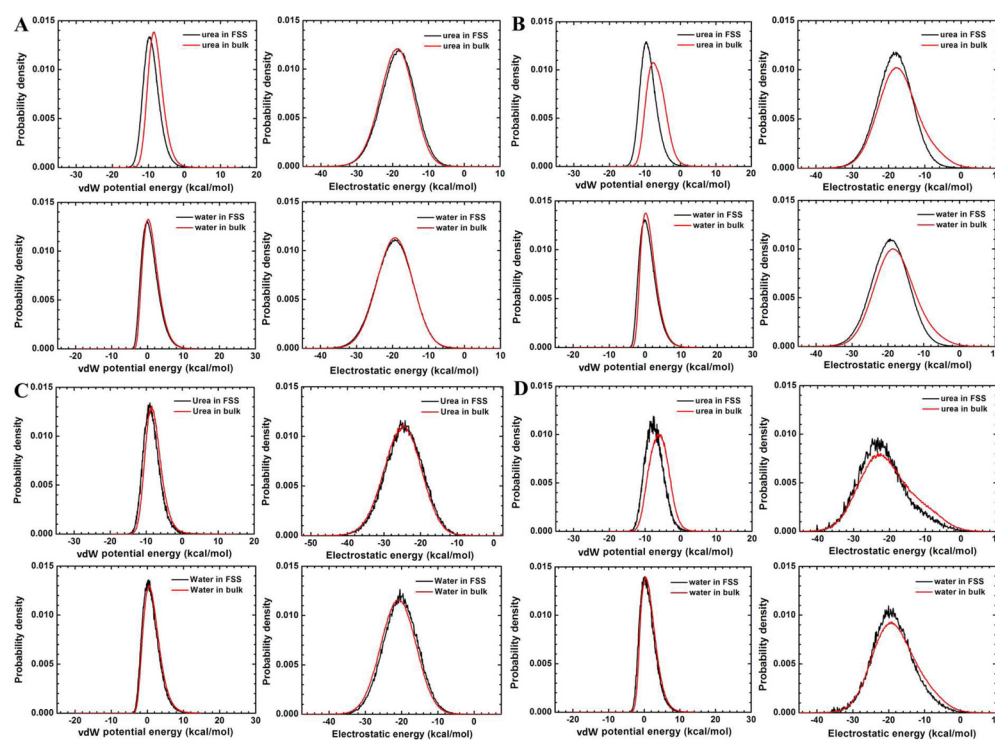


Figure 3. Comparison of the nonbonded interaction energy distributions of a solvent calculated with and without the periodic boundary conditions (PBC). A and B are cases for lysozyme with and without PBC, respectively; C and D are cases for NFGAIL peptide in 8 M urea with and without PBC, respectively.

Table 5. Comparison of Average Nonbonded Interaction Energies (in kcal/mol) of a Solvent Calculated with and without the Periodic Boundary Conditions (PBC), Taking the Lysozyme and NFGAIL Peptide as Examples^a

protein	solvent	with PBC			without PBC		
		ΔE_{elec}	ΔE_{vdW}	ΔE_{total}	ΔE_{elec}	ΔE_{vdW}	ΔE_{total}
lysozyme	urea	0.40	−1.23	−0.83	−1.32	−2.15	−3.47
	water	−0.15	−0.34	−0.49	−1.51	−0.38	−1.89
NFGAIL	urea	0.40	−0.59	−0.19	−1.43	−1.35	−2.78
	water	0.58	−0.36	0.23	−0.78	−0.36	−1.14

^a ΔE_{elec} , ΔE_{vdW} , and ΔE_{total} denote the differences in average electrostatic, vdW, and total interaction energies, respectively, for a solvent in first solvation shell of protein/peptide vs in bulk.

CONCLUSIONS

In a previous study,²⁷ we examined the mechanism of urea-induced denaturation of lysozyme and suggested that urea denatures proteins via direct dispersion-driven interactions with proteins. Here we perform large scale MD simulations of five representative protein/peptide systems in aqueous urea to further investigate the generality and robustness of the dispersion-interaction-driven mechanism. During the given simulation times, these proteins/peptide undergo global or partial unfolding. In all cases, accumulations of urea around backbones and side chains of proteins/peptide are observed, and the energetic analyses reveal that the accumulations mainly result from the stronger dispersion interactions of urea with proteins/peptide than water. Consistent with our previous case study of lysozyme, these findings suggest that urea denatures proteins via direct dispersion interactions, rather than electrostatic (hydrogen-bonded) interactions. Neither does it disrupt water structure as a “water breaker”. Further investigation demonstrates that the above mechanism is robust, independent of urea concentration and the force field used. Last, we emphasize the importance of periodic boundary conditions in pairwise energetic analyses. The present work provides a comprehensive study on the physical mechanism of urea-induced protein denaturation and suggests that the “dispersion-interaction-driven” mechanism should be common for all proteins.

ASSOCIATED CONTENT

Supporting Information

Detailed unfolding process for lysozyme, γ D-Crystallin, ubiquitin, and CI2 proteins. This material is available free of charge via the Internet at <http://pubs.acs.org>.

AUTHOR INFORMATION

Corresponding Author

*E-mail: ruhongz@us.ibm.com.

Notes

The authors declare no competing financial interest.

ACKNOWLEDGMENTS

We thank Xiaowei Tang, Weiqiu Zhu, Hangjun Lu, Zhen Xia, Seung-gu Kang, Pu Liu, and Payel Das for useful discussions and insightful comments. This work is partially supported by National Natural Science Foundation of China (Grant No. 30870593), the China Postdoctoral Science Foundation (Grant No. 2012M511351), Zhejiang Provincial Natural Science Foundation of China (Grant No. LY12A04007), and Fundamental Research Funds for the Central Universities. R.Z. acknowledges the financial support from the IBM BlueGene Program.

REFERENCES

- (1) Pace, C. N. *Methods Enzymol.* **1986**, *131*, 266–280.
- (2) Frank, H. S.; Franks, F. J. *Chem. Phys.* **1968**, *48*, 4746–4757.
- (3) Wetlaufer, D. B.; Coffin, R. L.; Malik, S. K.; Stoller, L. J. *Am. Chem. Soc.* **1964**, *86*, 508–514.
- (4) Hammes, G. G.; Schimmel, P. R. *J. Am. Chem. Soc.* **1967**, *89*, 442–446.
- (5) Chen, X.; Sagle, L. B.; Cremer, P. S. *J. Am. Chem. Soc.* **2007**, *129*, 15104–15105.
- (6) Sagle, L. B.; Zhang, Y. J.; Litosh, V. A.; Chen, X.; Cho, Y.; Cremer, P. S. *J. Am. Chem. Soc.* **2009**, *131*, 9304–9310.
- (7) Bennion, B. J.; Daggett, V. *Proc. Natl. Acad. Sci. U.S.A.* **2003**, *100*, 5142–5147.
- (8) England, J. L.; Pande, V. S.; Haran, G. *J. Am. Chem. Soc.* **2008**, *130*, 11854–11855.
- (9) Yang, L. J.; Gao, Y. Q. *J. Am. Chem. Soc.* **2010**, *132*, 842–848.
- (10) Wei, H. Y.; Fan, Y. B.; Gao, Y. Q. *J. Phys. Chem. B* **2010**, *114*, 557–568.
- (11) Cafilisch, A.; Karplus, M. *Struct. Fold. Des.* **1999**, *7*, 477–488.
- (12) Caballero-Herrera, A.; Nordstrand, K.; Berndt, K. D.; Nilsson, L. *Biophys. J.* **2005**, *89*, 842–857.
- (13) Robinson, D. R.; Jencks, W. P. *J. Am. Chem. Soc.* **1965**, *87*, 2462–2470.
- (14) Makhatazde, G. I.; Privalov, P. L. *J. Mol. Biol.* **1992**, *226*, 491–505.
- (15) Sharp, K. A.; Madan, B.; Manas, E.; Vanderkooi, J. M. *J. Chem. Phys.* **2001**, *114*, 1791–1796.
- (16) Auton, M.; Holthauzen, L. M. F.; Bolen, D. W. *Proc. Natl. Acad. Sci. U.S.A.* **2007**, *104*, 15317–15322.
- (17) Lim, W. K.; Rosgen, J.; Englander, S. W. *Proc. Natl. Acad. Sci. U.S.A.* **2009**, *106*, 2595–2600.
- (18) Klimov, D. K.; Straub, J. E.; Thirumalai, D. *Proc. Natl. Acad. Sci. U.S.A.* **2004**, *101*, 14760–14765.
- (19) Mountain, R. D.; Thirumalai, D. *J. Am. Chem. Soc.* **2003**, *125*, 1950–1957.
- (20) O'Brien, E. P.; Dima, R. I.; Brooks, B.; Thirumalai, D. *J. Am. Chem. Soc.* **2007**, *129*, 7346–7353.
- (21) Berteotti, A.; Barducci, A.; Parrinello, M. *J. Am. Chem. Soc.* **2011**, *133*, 17200–17206.
- (22) Canchi, D. R.; Paschek, D.; Garcia, A. E. *J. Am. Chem. Soc.* **2010**, *132*, 2338–2344.
- (23) Canchi, D. R.; Garcia, A. E. *Biophys. J.* **2011**, *100*, 1526–1533.
- (24) Stumpe, M. C.; Grubmuller, H. *J. Am. Chem. Soc.* **2007**, *129*, 16126–16131.
- (25) Stumpe, M. C.; Grubmuller, H. *PLoS Comput. Biol.* **2008**, *4*.
- (26) Lee, M. E.; van der Vegt, N. F. A. *J. Am. Chem. Soc.* **2006**, *128*, 4948–4949.
- (27) Hua, L.; Zhou, R. H.; Thirumalai, D.; Berne, B. J. *Proc. Natl. Acad. Sci. U.S.A.* **2008**, *105*, 16928–16933.
- (28) Li, W.; Zhou, R.; Mu, Y. *J. Phys. Chem. B* **2012**, *116*, 1446–1451.
- (29) Zangi, R.; Zhou, R. H.; Berne, B. J. *J. Am. Chem. Soc.* **2009**, *131*, 1535–1541.
- (30) Das, P.; Zhou, R. H. *J. Phys. Chem. B* **2010**, *114*, 5427–5430.
- (31) Xiu, P.; Yang, Z. X.; Zhou, B.; Das, P.; Fang, H. P.; Zhou, R. H. *J. Phys. Chem. B* **2011**, *115*, 2988–2994.

- (32) Zhou, R. H.; Li, J. Y.; Hua, L.; Yang, Z. X.; Berne, B. J. *J. Phys. Chem. B* **2011**, *115*, 1323–1326.
- (33) Das, A.; Mukhopadhyay, C. *J. Phys. Chem. B* **2009**, *113*, 12816–12824.
- (34) Whitney, P. L.; Tanford, C. *J. Biol. Chem.* **1962**, *237*, 1735–1737.
- (35) Wei, H. Y.; Yang, L. J.; Gao, Y. Q. *J. Phys. Chem. B* **2010**, *114*, 11820–11826.
- (36) Stumpe, M. C.; Grubmüller, H. *Biophys. J.* **2009**, *96*, 3744–3752.
- (37) Wallqvist, A.; Covell, D. G.; Thirumalai, D. *J. Am. Chem. Soc.* **1998**, *120*, 427–428.
- (38) Jha, S. K.; Udgaonkar, J. B. *Proc. Natl. Acad. Sci. U.S.A.* **2009**, *106*, 12289–12294.
- (39) Eleftheriou, M.; Germain, R. S.; Royyuru, A. K.; Zhou, R. H. *J. Am. Chem. Soc.* **2006**, *128*, 13388–13395.
- (40) Huang, X. H.; Hagen, M.; Kim, B.; Friesner, R. A.; Zhou, R. H.; Berne, B. J. *J. Phys. Chem. B* **2007**, *111*, 5405–5410.
- (41) Li, X.; Li, J. Y.; Eleftheriou, M.; Zhou, R. H. *J. Am. Chem. Soc.* **2006**, *128*, 12439–12447.
- (42) Zhou, R. H.; Berne, B. J.; Germain, R. *Proc. Natl. Acad. Sci. U.S.A.* **2001**, *98*, 14931–14936.
- (43) Zhou, R.; Huang, X.; Margulis, C. J.; Berne, B. J. *Science* **2004**, *305*, 1605–1609.
- (44) Phillips, J. C.; Braun, R.; Wang, W.; Gumbart, J.; Tajkhorshid, E.; Villa, E.; Chipot, C.; Skeel, R. D.; Kale, L.; Schulten, K. *J. Comput. Chem.* **2005**, *26*, 1781–1802.
- (45) MacKerell, A. D.; Bashford, D.; Bellott, M.; Dunbrack, R. L.; Evanseck, J. D.; Field, M. J.; Fischer, S.; Gao, J.; Guo, H.; Ha, S.; et al. *J. Phys. Chem. B* **1998**, *102*, 3586–3616.
- (46) Neria, E.; Fischer, S.; Karplus, M. *J. Chem. Phys.* **1996**, *105*, 1902–1921.
- (47) Jorgensen, W. L.; Maxwell, D. S.; TiradoRives, J. *J. Am. Chem. Soc.* **1996**, *118*, 11225–11236.
- (48) Hess, B.; Kutzner, C.; van der Spoel, D.; Lindahl, E. *J. Chem. Theory Comput.* **2008**, *4*, 435–447.
- (49) Duffy, E. M.; Severance, D. L.; Jorgensen, W. L. *Isr. J. Chem.* **1993**, *33*, 323–330.
- (50) Smith, L. J.; Berendsen, H. J. C.; van Gunsteren, W. F. *J. Phys. Chem. B* **2004**, *108*, 1065–1071.
- (51) Jorgensen, W. L.; Chandrasekhar, J.; Madura, J. D.; Impey, R. W.; Klein, M. L. *J. Chem. Phys.* **1983**, *79*, 926–935.
- (52) King, J. A.; Das, P.; Zhou, R. H. *Proc. Natl. Acad. Sci. U.S.A.* **2011**, *108*, 10514–10519.
- (53) Kong, F.; King, J. *Protein Sci.* **2011**, *20*, 513–528.
- (54) Hess, B.; Bekker, H.; Berendsen, H. J. C.; Fraaije, J. J. *Comput. Chem.* **1997**, *18*, 1463–1472.
- (55) Miyamoto, S.; Kollman, P. A. *J. Comput. Chem.* **1992**, *13*, 952–962.
- (56) Ryckaert, J. P.; Ciccotti, G.; Berendsen, H. J. C. *J. Comput. Phys.* **1977**, *23*, 327–341.
- (57) Gao, M.; She, Z.-S.; Zhou, R. *J. Phys. Chem. B* **2010**, *114*, 15687–15693.